MATERIALS & DESIGN **Volume:** 108 **Pages:** 618-623 **DOI:** 10.1016/j.matdes.2016.07.034

Effect of Ca addition on interface formation in Al(Ca)/Al_2O_3 composites prepared by gas pressure assisted infiltration.

M. Nosko[a*], Š. Nagy[a, b], L. Weber[c], I. Maťko[d], M. Mihalkovič[d], K. Iždinský[a], Ľ. Orovčík[a]

[a] Institute of Materials and Machine Mechanics, Slovak Academy of Sciences, Dúbravská cesta 9, 845 11 Bratislava, Slovak Republic

[b] Institute of Materials Science, Faculty of Material Sciences and Technology in Trnava, Slovak University of Technology in Bratislava, Slovakia

[c] Ecole Polytechnique Federale de Lausanne, Laboratory of Mechanical Metallurgy, Station 12 CH-1015, Lausanne, Switzerland

[d] Institute of Physics, Slovak Academy of Sciences, Dúbravská cesta 9, 845 11 Bratislava 45, Slovak Republic

[*]Corresponding author: Martin Nosko, E-mail: ummsnoso@savba.sk, Tel: +421 2 44254751

The aim of the work is to study interface formation between Al_2O_3 particles and Al(Ca) matrix in dependence of ~~the~~ Ca content. Aluminium matrix composites (AMC) subjected to investigation were prepared by gas pressure assisted infiltration of alumina beds with aluminium-calcium alloys. It is shown that ~~the~~ alumina particles in the AMC are covered with a monocalcium aluminates layer whose coherence increases with increasing amounts of Ca in the aluminium-calcium alloys. Moreover, Al4Ca intermetallic phases are formed with increasing Ca content that connect alumina particles together. XRD confirms the presence of both $CaAl_2O_4$ and $CaAl_4O_7$ ternary phases. However, HRTEM analysis confirmed $CaAl_2O_4$ with a rather complex structure containing a high density of stacking faults. It appeared that annealing at 735°C does improve consistency of interface for Al 2wt.-%Ca/Al_2O_3 AMC, but do not affect the thickness of the interface in dependence on annealing time.

Key words

Al_2O_3 particles, AlCa alloy, Gas pressure infiltration, Interface, Aluminum matrix composites

Introduction

Aluminium and its alloys exhibit an attractive combination of good corrosion resistance, low density and appropriate mechanical properties. When combined with appropriate reinforcing phases, metal matrix composite with desirable properties can be produced. Aluminium matrix composites (AMC) form a group of advanced materials due to their low density, high specific modulus, low coefficient of thermal expansion and good wear resistance. None of the existing conventional materials offers as favourable combination of properties as composites based on aluminium and its alloys [1-7]. Since stiffening and strengthening of metal matrix composites rely on load transfer across the interface, appropriate interfaces are desirable [1-5,7-13]. Uniform distribution of reinforcing particles within the matrix is another essential ingredient to avoid anisotropic properties, premature yielding in weak areas or damage nucleation in particle clusters [9].

Several manufacturing routes for preparation of the Al/Al_2O_3 AMCs have been developed over the years. These were on one hand essentially based on mechanical or gas pressure assisted infiltration (Squeeze casting and GPAI, respectively) to overcome capillary forces, and on the other hand foundry techniques using mechanical or electromagnetic stirring and thus mixing particles into the liquid metal [11, 14-17]. Nagy et al. [8] have proposed a new approach relying on the manufacturing of the AMC with desired amount of reinforcement using master alloy pellets with 50 vol. % of Al_2O_3 to be mixed with unreinforced melt.

As has been shown by several authors [2,12-13, 18-19], alloying of the aluminium or activation of the alumina surface before infiltration could improve wettability of the particles. This is due to the formation of the interfacial reaction layer between Al/Al_2O_3 which decreases the wetting angle and can contribute to improved uniformity of distribution of the reinforcement in the melt. Various alloying elements (Cu, Si, Mg, Ca, Sr, Ce, Li) have been investigated yet the main attention has been focused on the Al-Mg system due to the formation of $MgAl_2O_4$ spinel interface [2,4,11-13,20-23]. Levi et al. even suggest that the formation of spinel at the interface between aluminium alloy and Al_2O_3 is crucial for the formation of strong bonds between particles and matrix [12]. Further, it has been reported that the wetting angle can be reduced also by Ni coating of alumina particles prior to infiltration. This however, leads to formation of interfacial intermetallic phases [7]. Nizhenko and Floka [20] studied the wettability of different types of alumina with aluminium alloys containing various amounts of Si, Cu and Ni. Actually, no significant effect of these three constituents has been recognized. However, a significant drop in contact angle occurred at temperatures in excess of 900 to 1000 °C associated with the evaporation of surface oxide layer on the melt.

In spite of the fact that calcium is chemically very similar to Mg and that it forms with aluminium five different mixed oxides ($CaAl_2O_4$, $CaAl_4O_7$, $CaAl_{12}O_{19}$, $Ca_3Al_2O_6$ and $Ca_{12}Al_{14}O_{33}$) [4-10, 28-34, 40] the effect of Ca on the interface formation between Al/Al_2O_3 has to our knowledge not been studied for metallic system. The present contribution hence aims at elucidating the effect of Ca-addition to aluminium on the interface formation in $Al(Ca)/Al_2O_3$ composites in order to improve the particle-matrix bonding.

Experimental

The AMC were prepared by gas pressure assisted liquid metal infiltration [25-26]. Prior to infiltration, Al_2O_3 powder particles were annealed at 950°C for 2 h in air to increase their wettability due to dehydroxylation of the powders and changes at the powder surface [2]. Subsequently, packed beds of commercial alumina powder AMDRY 6060 (Sulzer Metco Europe GmbH) with particle size of 45 μm were infiltrated at the temperature of 950 °C and 4 MPa argon pressure with aluminium alloys containing various amounts of Ca (1, 2 and 4 wt.-%). Cooling at the rate of 20 °C/min until solidification was applied. Subsequent cooling up to the room temperature has been adopted at the rate of approximately 8 °C/min.

To study microstructural changes during annealing, the aluminium alloy with 2 wt.-%Ca was annealed at 735°C for 1, 4 and 8 hours in air.

The microstructure of the master alloy composites with variable Ca-content was investigated with a FEG-SEM 7600F equipped with EDS (X-max 50mm^2, Oxford Instruments Ltd.). Based on the Monte Carlo simulations of electron trajectory in solids via Casino v2.48 [27], acceleration voltage was set to 7,2 kV to suppress the side effect of the x-ray signal from the interaction volume and thus improve the EDS measurement accuracy.

Transmission electron microscopy (TEM) and high-resolution transmission electron microscopy (HR-TEM) measurements were performed using JEOL 2000FX and JEOL 2100F microscopes operated at 200 kV to reveal the interface between Al_2O_3 and Al alloy and to identify the interfacial phases within. The microscope JEOL 2100F was equipped with an image-side Cs-corrector, EDX detector (Oxford Instruments) and delivered lateral resolution of better than 1.4 A. Thin foils were prepared for the TEM studies using mechanical grinding followed by ion milling with a GATAN PIPS II machine.

MATERIALS & DESIGN **Volume:** 108 **Pages:** 618-623 **DOI:** 10.1016/j.matdes.2016.07.034

To support identification of the interfacial phases, X-ray diffraction (XRD) using a Bruker AXS D4 Endeavor diffractometer with Bragg–Brentano geometry and Cu Kα radiation at λ=0.15406 nm was conducted.

Results and discussion

Microstructure

SEM micrograph of the AMC Al-x-wt. % Ca/Al_2O_3 (x=1, 2, 4) after pressure-assisted infiltration is shown in Fig.1. The volume fraction of the alumina is approximately 50%, which is in good agreement with previously reported results [8]. In general, the microstructure consists of the Al_2O_3 particles uniformly distributed in aluminium matrix. However, there are some voids in the matrix, cracked Al_2O_3 particles and occasional occurrence of micropores on the Al(Ca)/Al_2O_3 interface can be observed. To avoid the presence of gas between the particles, the vacuum was pulled in the powder bed to pressure 100 Pa prior to infiltration. Moreover, infiltration was performed at relatively high pressure (4 MPa), and the cooling was performed under pressure as well to avoid shrinkage. Nevertheless, shrinkage porosity cannot be completely excluded in the final stages of solidification where local residual liquid is no longer in contact with the pressurized liquid.

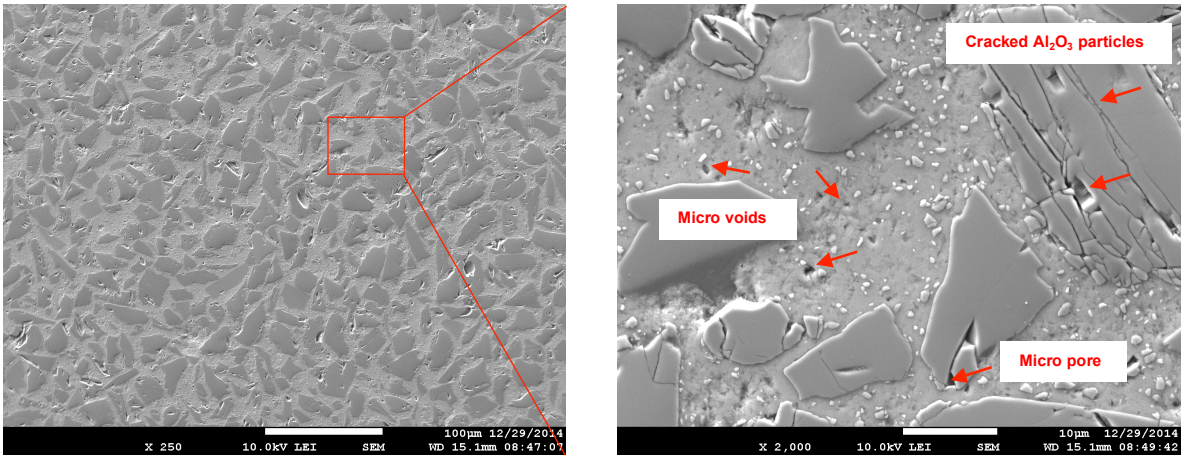

(a) (b)

Fig. 1. SEM microstructure of Al (1wt.-%Ca)/Al_2O_3 in different magnifications; (a) uniform distribution of Al_2O_3 particles in aluminium matrix and (b) enlarged area with defects within microstructure.

EDS maps revealing the distribution of Ca are presented in Fig. 2. As can be seen, there is an increasing amount of eutectic microstructure in rough agreement with the phase diagram predicting 12, 25 and 50 vol.-% of eutectic for alloys of 1, 2 and 4 wt.-% Ca, respectively. Furthermore, the alumina particles seem to be delineated with a thin layer enriched in Ca (confirmed also by EDS - TEM), being more pronounced as the Ca content increases. Previous studies had indicated presence of $CaAl_2O_4$, $CaAl_4O_7$, $CaAl_{12}O_{19}$, $Ca_3Al_2O_6$ and $Ca_{12}Al1_{14}O_{33}$ within microstructure in case of ceramic mixtures [28-35]. Moreover, some of them also in case of manufacturing the aluminium foams with Ca addition [35-37]. Both are in agreement with expectations based on thermodynamics. From total energy calculations using the first principles package VASP [38-39], formation enthalpies for the ternary AlCaO compounds are in the range -3.2 to -3.3 eV/atom (as compared to formation enthalpies -2.8 and -3.1 eV/atom for Al_2O_3 and CaO respectively), and thus predict stability of the candidate ternary phases. Therefore, formation of the ternary AlCaO phase at interface is also

natural for metallic system, which is supported by XRD measurements shown in Fig. 3. The phase in the eutectic regions gives an Al:Ca ratio of roughly 4:1, which corresponds to the Al_4Ca phase expected from the phase diagram and as confirmed in XRD (Fig. 3). According to calculations of the amount of Al_4Ca as provided by INCA energy + (Oxford Instruments Ltd.) which is used for EDS evaluation, the amount of Al4Ca increased from 1.7 vol.-pct to 8.5 vol.-pct and 14.8 vol.-pct in alloys with 1, 2, and 4 wt.-pct. Ca, respectively.

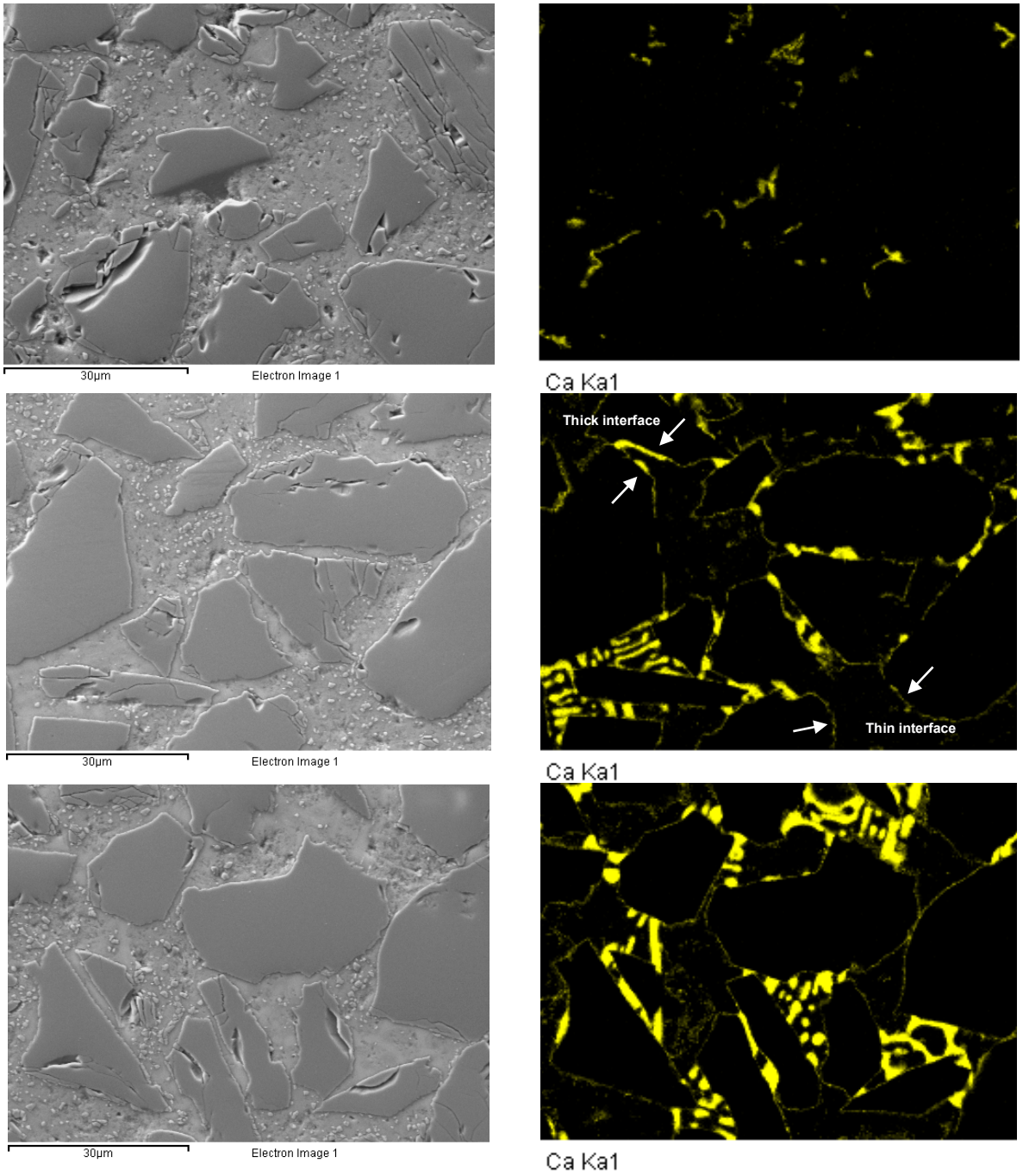

Fig. 2. EDS maps revealing the distribution of Ca for all three matrix alloy compositions; (top) Al 1wt.-%Ca (middle) Al 2wt.-%Ca and (bottom) Al 4 wt.-%Ca.

The Gibbs free energy of the ternary AlCaO phase is relatively high which suggests formation of the ternary phases on the Al/Al_2O_3 interface. This is also supported by XRD measurements as seen in

Fig. 3. XRD measurements suggest presence of $CaAl_2O_4$, which was also observed in previous studies in case of ceramics compounds e.g. combination of α-Al_2O_3 and $CaCO_3$, where formation temperature is approximately 1100°C [28-31]. In our case, the $CaAl_2O_4$ was formed at lower temperature 950°C than previously reported in [28-31]. They reported, that $CaAl_2O_4$ phase coexists with $Ca_{12}Al_{14}O_{33}$ if it is formed at high temperature synthesis from ceramic compounds (α-Al_2O_3 and $CaCO_3$). However, formation of the $Ca_{12}Al_{14}O_{33}$ was not revealed in our study, probably due to lower temperature or significantly different initial conditions. Moreover, we have not observed other thermodynamically stable phases potentially formed in the α-Al_2O_3 and CaO system after sintering such as $CaAl_{12}O_{19}$, $Ca_3Al_2O_6$ and $Ca_{12}Al1_{14}O_{33}$ [32]. However XRD suggests also formation of $CaAl_4O_7$.

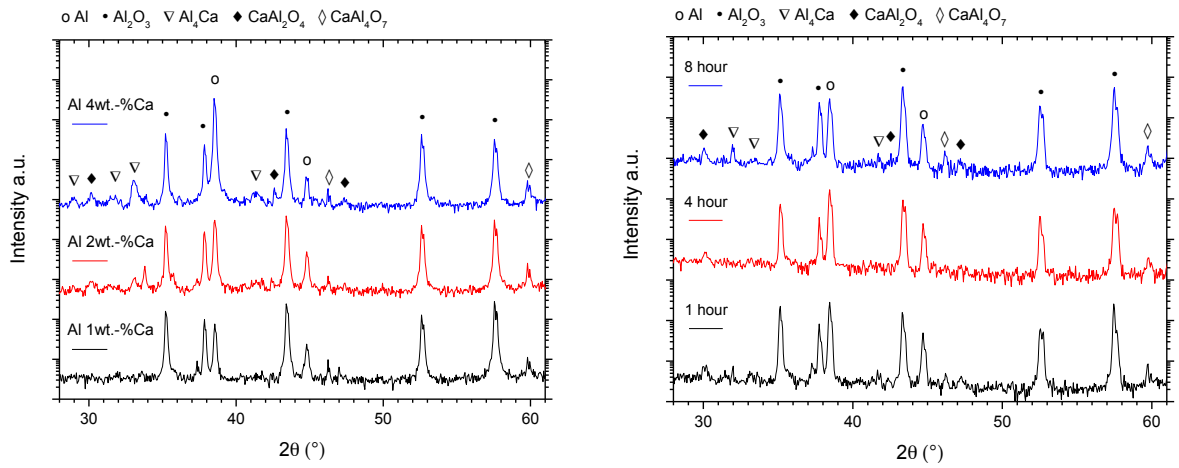

Fig. 3. XRD diffraction in dependence on (a) Ca amount in aluminium alloy and (b) on annealing condition for Al 2wt.-pct Ca/Al_2O_3, temperature of annealing was 735°C.

As shown in Fig. 4 a-f, TEM investigation confirmed the presence of a Ca containing layer at the Al-x-wt.-pct Ca/Al_2O_3 (x=1, 2, 4) interface. High-resolution analysis shown in Fig. 4g and h reveals a rather complex structure containing dense occurrence of stacking faults. The typical distance between stacking fault planes is approximately 5 nm. Their orientation is roughly perpendicular to the interface with Al_2O_3 crystals, which suggests that fault generation is a consequence of misfit of lattice parameters of the structures and can result in formation of a semi-coherent interface as seen in Fig. 4g. Exact interpretation of high resolution micrographs is rather complicated in this case, certain areas further away from the interface with Al_2O_3 crystals (with lower density of structure faults) allow plane indexing corresponding to the -monocalcium aluminate $CaAl_2O_4$ (PDF no. 23-1036) as seen in Fig. 4h. The thickness of the interface does not change in dependence on Ca amount in matrix alloy and can be estimated to approximately 200 - 300 nm as documented in Fig. 4 a-f.

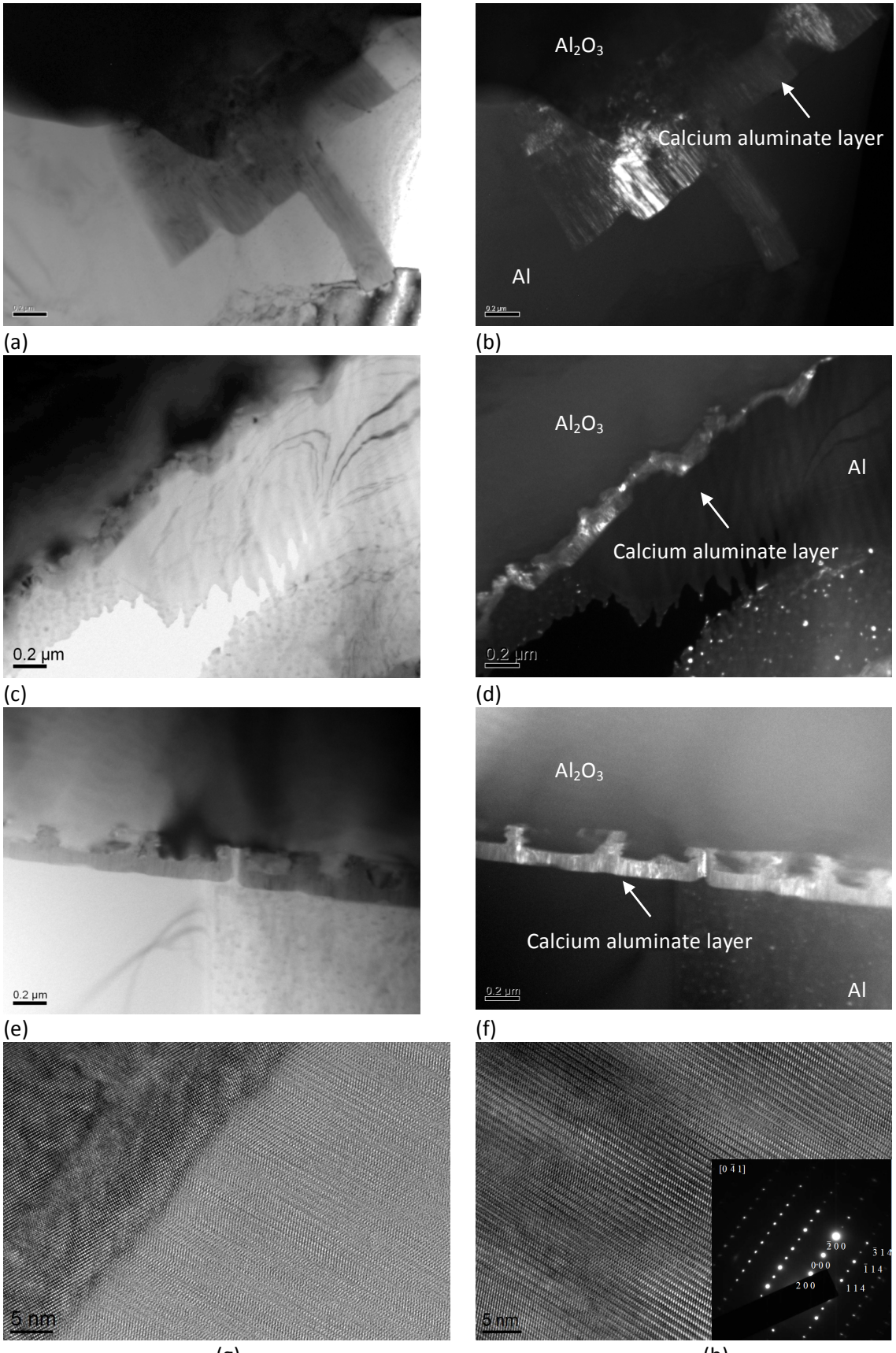

Fig.4 . TEM micrographs of the Al 1wt.-%Ca/Al_2O_3 interface in light (a) and dark field (b); Al 2wt.-%Ca/Al_2O_3 interface in light (c) and dark field (d); Al 4wt.-%Ca/Al_2O_3 interface in light (e) and dark field (f); HR-TEM micrographs of the interface (g) and interfacial compound $CaAl_2O_4$ with diffraction pattern (h).

The effect of annealing on the stability of Al 2wt.-pct.Ca/Al_2O_3 interface is presented in Fig. 5. There is a significant difference in Ca distribution within the microstructure before and after annealing as documented in Fig. 2 and Fig. 5 respectively. In the case of annealing, the consistency of the interface is improved for certain amount of Ca in Al alloy (Al 2wt.-%Ca) and more cracks can be observed at the interface and in Al_2O_3 particles as revealed in Fig. 5 middle row. Moreover, increase of annealing time does not affect the thickness of the Al 2wt.-pct. Ca/Al_2O_3 interface.

However, if one compares the XRD data of no-treated and heat-treated samples (Fig. 3), there are no significant differences between peaks of $CaAl_2O_4$ and $CaAl_4O_7$. Therefore, we assume that the interface is formed as previously mostly by $CaAl_2O_4$ and $CaAl_4O_7$. However, the area of eutectic region is significantly decreased in comparison with no-treated AMC (Fig. 5), which suggests the decrease of overall Al_4Ca amount. This assumption is confirmed by XRD measurement shown in Fig. 3b. Since Ca has a high affinity to oxygen, it was withdrawn towards AMC surface during annealing and its amount in inner structure ~~is~~ therefore significantly decreases.

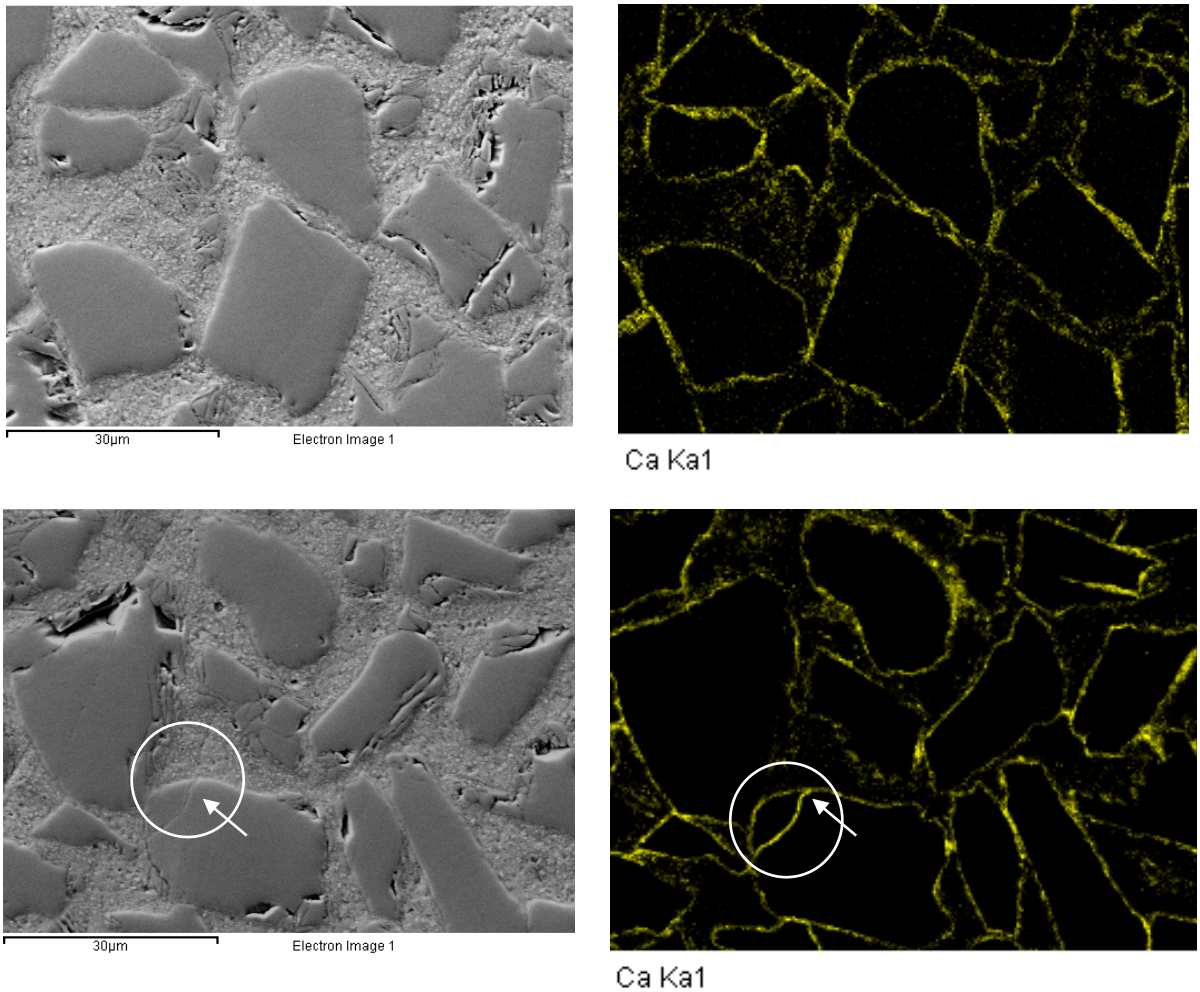

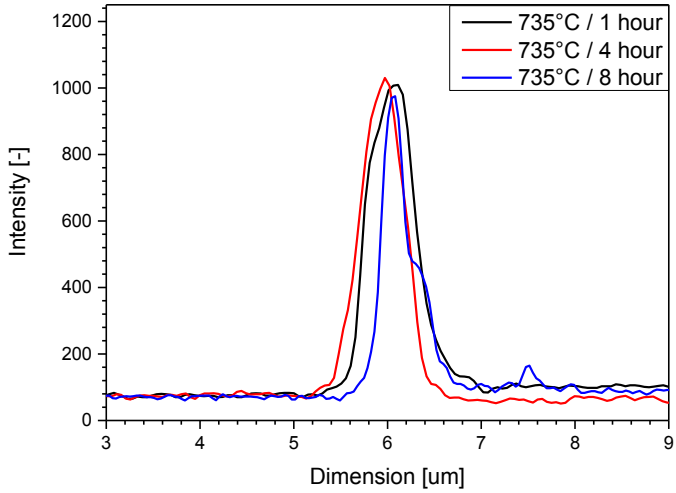

Fig. 5. EDS maps revealing the distribution of Ca in Al 2wt.-%Ca /Al_2O_3 depending on the annealing conditions; (top row) 735°C/1 hour, (middle row) 735°C/8 hours and (bottom row) reveal thickness of interfacial layer through EDS linescan.

Conclusion

In the present work, interface formation between Al_2O_3 and Al(Ca) alloys in dependence on Ca amount during gas-pressure assisted infiltration has been studied. It was shown that:

- Ca addition in aluminium alloy results in formation of the interfacial layer between Al and Al_2O_3 in AMC, which becomes more compact with increasing amount of Ca.

- The thickness of the interfacial phase does not change in with the Ca content but the amount of the Al_4Ca phases between Al_2O_3 particles increases.

- XRD indicates the presence of $CaAl_2O_4$ and $CaAl_4O_7$ ternary phases within microstructure. High-resolution micrographs reveal $CaAl_2O_4$ at interface.

- Subsequent annealing of AMC at 735°C results improved consistency of interfacial layer in case of Al 2wt.-%Ca AMC and decrease of the Al_4Ca amount. Effect of annealing time on interfacial layer changes was not observed.

Acknowledgement

This work was supported by Slovak Foundation VEGA grant 2_0158_16, and by grant APVV-14-0936. Devices from European project ITMS 26240120006 were used for this work. The authors would like to thank to Dr. P. Švec for help with X-ray measurements.

References

[1] Surappa M K, Rohatgi P K. Preparation and properties of cast aluminium–ceramic particle composites. J. Mater. Sci. 1981;16:983-93.

[2] Shorowordi K M, Laoui T, Haseeb A S M A, Celis J P, Froyen L. Microstructure and interface characteristics of B4C, SiC and Al2O3 reinforced Al matrix composites: a comparative study. J. Mater. Process. Tech. 2003;142:738-43.

[3] Oh S Y, Cornie J A, Russel K C. Wetting of ceramic particulates with liquid aluminium alloys. Part I. Experimental techniques. Metall. Trans. A 1989;20:527-32.

[4] Kevorkijan V M, Torkar M, Šuštaršič B. Modeling of the reactive immersion of ceramic particles into molten aluminium alloys. Compos. Sci. Technol. 1999;59:1503-11.

[5] Durai T G, Das K, Das S. Synthesis and characterization of Al matrix composites reinforced by in situ alumina particulates. Mater. Sci. Eng. A 2007;445-446:100-5.

[6] Ezatpour H R, Sajjadi S A, Sabzevar M H, Huang Y Z. An investigation of the tensile and compressive properties of Al6061 and its nanocomposites in as-cast and extruded condition, Mater. Sci. Eng. A 2014, 607:589-95

[7] León C A, Drew R A L. The influence of nickel coating on the wettability of aluminum on ceramics. Compos. Part A-Appl. S. 2002;33:1429-32.

[8] Nagy S, Nosko M, Orovčík Ľ, Iždinský K, Kúdela S, Krížik P. Pre-review study of the aluminum/alumina master alloy made through pressure infiltration. Mater. Design 2015;66:1-6.

[9] Chen X H, Hong Y. Solid-liquid interface dynamics during solidification of Al7075-Al_2O_{3np} based metal matrix composites, Mater. Design 2016; 94: 148-158.

[10] Dyzia M, Dolata A J, Boczkal S. Structure of interface between matrix alloy and reinforcement particles in Al/SiCp + Cgp hybrid composites, Mater. Today 2016; 3:235-9.

[11] Li Y, Li Q, Liu W, Shu G. Effect of Ti content and stirring time on microstructure and mechanical behaviour of Al-B4C composites, J. Alloys Compds 2016, 684:496-503

[12] Levi C G, Abbaschian G J, Mehrabian R. Interface interaction during fabrication of aluminum alloy‐alumina fiber composites. Metall. Trans. A 1978;9:697-711.

[13] Lebeau T, Strom-Olsen J O, Gruzleski J E, Drew R A L. Aluminum alloy/alumina-based ceramic interactions. Mater. Charact. 1995;35:11-22.

[14] Shabani M O, Mazahery A. Application of GA to optimize the process conditions of Al matrix composites, Compos. Part B-Eng. 2013; 45:185-91

[15] Léger A, Weber L, Mortensen A. Influence of the wetting angle on capillary forces in pressure infiltration, Acta Mater. 2015; 91:57-69

[16] Tofigh A A, Rahimipour M R, Shabani M O, Davami P. Application of the combined neuro-computing, fuzzy logic and swarm intelligence for optimization of compocast nanocomposites. J. Compos. Mater. 2014;0:1-11.

[19] Shabani M O, Rahimipour M R, Tofigh A A, Refined microstructure of compocast nanocomposites: the performance of combined neuro-computing, fuzzy logic and particle swarm techniques. Neural Comput. Appl. 2015;26:899-909.

[18] Laurent V, Chatain D, Chatillon C, Eustathopoulos N. Wettability of monocrystalline alumina by aluminum between its melting point and 1273 K. Acta Metall. Mater. 1988;36:1797-803.

[19] Donald J E, Eberhart J G. Adhesion in aluminium oxide-metal systems. T. Metall. Soc. AIME, 1965;233:512-7.

[20] Nakae H, Wu S. Engulfment of Al_2O_3 particles during solidification of aluminum matrix composites. Mat. Sci. Eng. A 1998;252:232-8.

[21] Munitz A, Metzger M, Mehrabian R. The interface phase in Al-Mg/Al_2O_3 Composites. Metall. Trans. A 1979; 10:1491-7.

[22] Hall I W, Barrailler V. The effect of thermal exposure on the mcrostructure and fiber/matrix interface of an Al_2O_3/Al composite. Metall. Trans. A 1986;17:1075-80.

[23] Chappleman G R, Watts J F, Clyne T W. The interface region in squeeze-infiltrated composites containing δ-alumina fibre in an aluminium matrix. J. Mater. Sci. 1985;20:2159-68.

[24] Nizhenko V I, Floka L I. Wetting of Al_2O_3-Based Oxide Ceramics by Molten Aluminum. Powder Metall. Met. C+ 2001;40:271-6.

[25] Kouzeli M, Mortensen A. Size dependent strengthening in particle reinforced aluminium. Acta Mater. 2002;50:39-51.

[26] Weber L, Dorn A, Mortensen A. On the electrical conductivity of metal matrix composites containing high volume fractions of non-conducting inclusions. Acta Mater. 2003;51: 3199–211.

[27] http://www.gel.usherbrooke.ca/casino/

[28] Róg G, Kozlowska-Róg A, Zakula-Sokól K, Borchardt G. Determination of the standard Gibbs free energies of formation of the calcium aluminates from the oxides by e.m.f. measurements. J. Chem. Thermodyn. 1993;25:807-10.

[29] Yi S, Huang Z, Huang J, Fang M, Liu Y, Zhang S. Novel calcium hexaluminate/spinel-alumina composites with graded microstructures and mechanical properties. Sci. Rep. 2014; 4333:1-7.

[30] Rivas Mercury J M, Aza A H D. Pena P. Synthesis of CaAl2O4 from powders: Particle size effect. J. Eur. Ceram. Soc. 2005;25:3269-79.

[31] Iftekhar S, Grins J, Svensson G, Lööf J, Jarmar T, Botton G A, Andrei C M, Engqvist H. Phase formation of $CaAl_2O_4$ from $CaCO_3$–Al_2O_3 powder mixtures. J. Eur. Ceram. Soc. 2008;28:747-56.

[32] Zawrah M F, Khalil N M. Synthesis and characterization of calcium aluminate nanoceramics for new applications. Ceram. Int. 2007;33:1419-25.

[33] Lazić B, Kahlenberg V, Konzett J, Kaindl R. On the polymorphism of $CaAl_2O_4$—structural investigations of two high pressure modifications. Solid State Sci. 2006;8:589-97.

[34] Ma Ch, Kampf A R, Connolly H C, Beckett J R, Rossman G R, Sweeneys-Smith S A, Schrader D L. Krotite, CaAl2O4, a new refractory mineral from the NWA 1934 meteorite. Am. Mineral. 2011;96:709-15.

[35] Banhart J. Manufacture, characterisation and application of cellular metals and metal foams. Prog. Mater. Sci. 2001;46:559-632.

[36] Onck P R, Van Merkerk R, Raaijmakers A, De Hosson J Th M. Fracture of open- and closed-cell metal foams. J. Mater. Sci. 2005;40: 5821-8.

[37] Sugimura Y, Meyer J, He M Y, Bart-Smith H, Grenstedt J, Evans A G. On the mechanical performance of closed cell Al alloy foams. Acta Mater. 1997;45:5245-59.

[38] Kresse G, Hafner J. Ab initio molecular dynamics for liquid metals. Phys. Rev. B 1993;47:558-61.

[39] Kresse G, Furthmuller J. Efficient iterative schemes for ab initio total-energy calculations using a plane-wave basis set. Phys. Rev. B 1996;54:11169-86.

[40] Shiri S, Abbasi M H, Monshi A, Karimzadeh F. Synthesis of the $CaAl_2O_4$ nanoceramic compound using high-energy ball milling with subsequent annealing, Adv. Powder Technol. 2014;25:338-41.